ORGANOMETALLICS

Article

pubs.acs.org/Organometallics

Metalloradical-Catalyzed Selective 1,2-Rh-H Insertion into the Aliphatic Carbon−Carbon Bond of Cyclooctane

Yun Wai Chan,[†] Bas de Bruin,*[,‡] and Kin Shing Chan*[,†]

[†]Department of Chemistry, The Chinese University of Hong Kong, Shatin, New Territories, Hong Kong, People's Republic of China

[‡]Van't Hoff Institute for Molecular Sciences (HIMS), University of Amsterdam, Science Park 904, 1098 XH, Amsterdam, The Netherlands

Supporting Information

ABSTRACT: The selective aliphatic carbon−carbon activation of cyclo-octane (c-octane) was achieved via the Rh^{II}(ttp)-catalyzed 1,2-addition of Rh(ttp)H to give Rh(ttp)(n-octyl) (ttp = tetratolylporphyrinato dianion) in good yield under mild reaction conditions. This mechanism is further supported by DFT calculations. The reaction worked only with the sterically accessible Rh(ttp) porphyrin complex but not with the bulky Rh(tmp) system (tmp = tetrakismesitylporphyrinato dianion), thus showing the highly steric sensitivity of carbon−carbon bond activation by transition metal complexes.

INTRODUCTION

Alkane functionalization in a homogeneous medium is an important and challenging process which involves either carbon−hydrogen bond activation (CHA)[1] or carbon−carbon bond activation (CCA)[2] with organic, inorganic, and organometallics reagents followed by functionalization. Although aliphatic C−C bonds are weaker than aliphatic C−H bonds, CCA of alkanes by the attack of a transition metal complex is much less reported due to steric hindrance of the carbon atoms which are shielded by peripheral C−H bonds as well as for statistical reasons associated with C−C bonds being typically less abundant than C−H bonds in organic compounds.[3]

Cyclo-octane (c-octane) is a relatively unstrained cycloalkane with a strain energy of 9.6 kcal/mol[4] and therefore serves as a commonly studied substrate in alkane functionalization, mostly involving CHA. Some examples of CHA of c-octane are the iridium(I) pincer dihydride-catalyzed dehydrogenation to c-octene,[5a] the $FeCl_3$-catalyzed aerobic oxidation to c-octanol and c-octanone[5b] as well as the MnO_2-catalyzed bromination to c-octyl bromide.[5c]

Reports of CCA of c-octane are rare. CCA of c-octane in a heterogeneous medium requires a very high reaction temperature of 530 °C and consequently results in both CHA and CCA.[3a] Oxidative CCA of c-octane catalyzed by N-hydroxyphthalides/Co(II)/Mn(II) at 100 °C in 14 h gives ω- dicarboxylic acids in 2% yield only together with the major products being c-octanol and c-octanone.[3b]

We have recently discovered the base-promoted CHA of cyclic alkanes with Rh(III) porphyrins.[6] In contrast to c-pentane[6] and c-hexane,[6] c-heptane[7] undergoes both CHA and CCA to give Rh(III) porphyrin c-heptyl and benzyl.[7] Both CHA and CCA have been proposed to involve Rh(II) porphyrin as a reagent or as a catalyst. These Rh(II) porphyrins are unique metalloradicals and exhibit rich chemistry in bond activations including CHA[8,9] and CCA.[10,11] The bimetalloradical CHA of methane and toluene, based on the second order dependence of the Rh^{II}(tmp) (tmp = tetrakismesitylporphyrinato dianion) concentration in the rate laws, has been reported by Wayland et al.[8] The CCA mechanism has been shown to be dependent on Rh^{II}(tmp) concentration, with a first order rate dependence in both the reaction with nitroxide,[10] and in the reaction with 2-methyl substituted nitrile[11] and second order dependence in the reaction with cyclophane.[12] We have previously communicated the CCA of c-octane via the 1,2-addition of its carbon−carbon bond to Rh(ttp)H, catalyzed by the Rh^{II}(ttp) (ttp = tetratolylporphyrinato dianion) metalloradical to give Rh(ttp) n-octyl selectively[13] (Scheme 1) and now report our full studies and theoretical calculations.

Scheme 1. Metalloradical Catalyzed CCA of c-Octane with MH

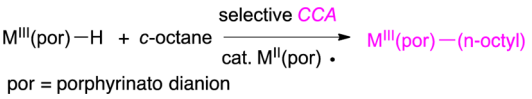

RESULTS AND DISCUSSION

Discovery and Optimization of CCA. Initially, c-octane was found to react poorly with Rh(ttp)Cl **1** to give Rh(ttp)(c-octyl) **2** and Rh(ttp)(n-octyl) **3** in 5% and 8% yields, respectively (Table 1, entry 1). A 72% yield of Rh(ttp)Cl **1** was recovered, and a trace amount of Rh(ttp)H **4** was observed. Both CHA and CCA products formed but the reaction was inefficient. Upon addition of KOH (10 equiv) to the reaction mixture, Rh(ttp)(c-octyl), Rh(ttp)(n-octyl), and Rh(ttp)H were obtained in 6%, 25%, and 62% yields, respectively in 7.5 h (Table 1, entry 2). When K_2CO_3 (10 equiv) was added,[9] Rh(ttp)Cl was consumed in 7.5 h, and Rh(ttp)(n-octyl) **3** and

Received: March 4, 2015

DOI: 10.1021/acs.organomet.5b00183
Organometallics XXXX, XXX, XXX−XXX

Table 1. Reaction of *c*-Octane with Rh(ttp)Cl 1

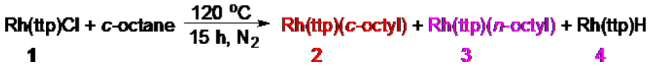

			yield (%)				
entry	additive[a]	time	1[b]	2	3	4	total
1		2 d	72	5	8	0	85
2	KOH	7.5 h	0	6	25	62	93
3	K_2CO_3	7.5 h	0	0	33	58	91

[a]10 equiv. [b]Recovery.

Rh(ttp)H **4** were obtained in 33% and 58% yields, respectively (Table 1, entry 3). The CCA product **3** is the formal 1,2-addition product of Rh(ttp)H **4** into the carbon−carbon bond of *c*-octane. The *c*-octane sample was pure and found to be free of *n*-octane and 1-octene by GC-MS analysis. Complexes **2** and **3** were independently synthesized by reductive alkylation with $NaBH_4$/R-Br (eq 1). Therefore, Rh(ttp)(*n*-octyl) **3** was confirmed as the CCA product of *c*-octane with its X-ray crystal structure communicated.[13]

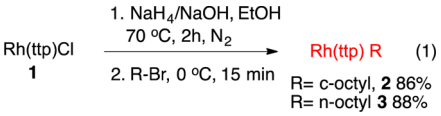

Mechanistic Investigation: CHA as An Intermediate for CCA? In some CCAs of hydrocarbons with transition metal complexes, the CCA can be a parallel[14a] and/or consecutive reaction channel[14] with CHA. We thus investigated whether the CHA product is an intermediate for CCA. Rh(ttp)(*c*-octyl) **2** was heated in benzene-d_6 in both neutral and basic conditions separately. Without K_2CO_3, Rh(ttp)(*c*-octyl) **2** gave Rh(ttp)(*n*-octyl) **3**, Rh(ttp)H **4**, and *c*-octene **5** in 10%, 76%, and 36% yields, respectively, after 21 h (Table 2). In the presence of

Table 2. Reaction Progress of the Thermal Reaction of Rh(ttp)(*c*-octyl) 2

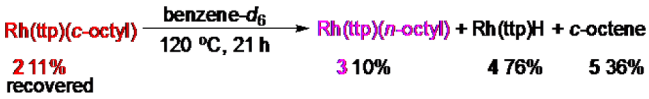

	yield %					
time (h)	2	3	4	5	total Rh	total org
0	100	0	0	0	100	0
1	87	0	11	9	98	96
21	11	10	76	36	97	57

K_2CO_3 (10 equiv), Rh(ttp)(*n*-octyl) **3** was isolated in a higher yield of 21% in 16 h with **2** recovered in 30% yield together with 42% yield of *c*-octene (Table 3). However, both reactions were low yielding and incomplete. We propose that the small amount of **3** is formed from a multistep pathway. The slow β-H elimination of **2** gives Rh(ttp)H **4** and octene. The slow homolysis of **2** gives Rh(ttp) and the *c*-octyl radical which undergoes disproportionation to give *c*-octane and *c*-octene. *c*-Octane can then further react with Rh(ttp)H to Rh(ttp)-*n*-octyl **3** (see discussion below). Therefore, CHA product **2** is unlikely a major intermediate leading to CCA product **3** and is more reasonably a parallel reaction product.

Reaction Profile with Rh(ttp)Cl. To gain further mechanistic understanding in order to enhance the CCA

Table 3. Reaction Progress of Rh(ttp)(*c*-octyl) 2 with K_2CO_3

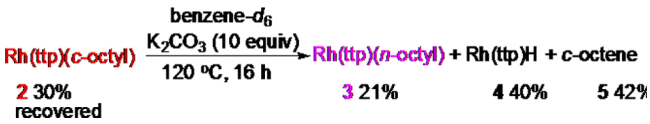

	yield %					
time (h)	2	3	4	5	total Rh pdt	total org pdt
0	100	0	0	0	100	100
0.5	97	00	0	0	97	97
1.5	80	100	18	20	98	100
2.5	73	100	24	25	97	98
10	36	16	41	40	93	92
16	30	21	40	42	91	93

reaction of Rh(ttp)Cl **1** with *c*-octane, the reaction was monitored by ^{1}H NMR spectroscopy in a sealed NMR tube with excess *c*-octane and K_2CO_3 in benzene-d_6 (Table 4).

Table 4. Reaction Progress of Rh(ttp)Cl with *c*-Octane with K_2CO_3

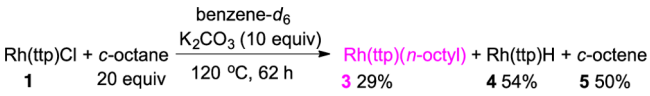

	yield %						
time (h)	1	3	4	5	6[a]	total Rh	total org
0	100	0	0	0	0	100	0
0.5	100	0	0	0	0	100	0
1	100	0	0	0	0	100	0
4.5	82	0	0	0	13	95	0
17	0	0	21	18	62	83	18
62	0	29	54	50	0	83	79
76	0	26	56	52	0	82	78
240	0	26	53	48	0	79	74

[a]**6** = $Rh_2(ttp)_2$.

Initially, Rh(ttp)Cl was first converted to $Rh_2(ttp)_2$ **6** in the presence of K_2CO_3.[15] At 4.5 h, 82% yield of Rh(ttp)Cl remained, while $Rh_2(ttp)_2$ **6** was formed in 13% yield. After 17 h, Rh(ttp)Cl was completely consumed. $Rh_2(ttp)_2$ **6**, Rh(ttp)H **4**, and *c*-octene **5** were formed in 62%, 21%, and 18% yields, respectively. After 62 h, $Rh_2(ttp)_2$ **6** completely reacted. The yields of Rh(ttp)H **4** and *c*-octene increased to 54% and 50%, respectively, and only 29% yield of CCA product Rh(ttp)(*n*-octyl) **3** was obtained. Finally, Rh(ttp)(*n*-octyl) **3** was generated in prolonged heating of 62 h, and still, Rh(ttp)H was consumed slowly and mostly remained unreacted even after 10 days. Therefore, both $Rh_2(ttp)_2$ and Rh(ttp)H are possible intermediates. The observed red gummy residue showing ^{1}H NMR upfield signals at $\delta = -5$ to 1 ppm were assigned to Rh(ttp)-incorporated *c*-octene oligomers (about 15% NMR yield), which indicate the occurrence of Rh^{II}(ttp)-initiated oligomerization of *c*-octene.[16,17] We did not pursue the examination of the detailed structures of these oligomers. The formation of *c*-octene, which forms from the β-H elimination of Rh(ttp)(*c*-octyl) **2**, indicates the occurrence of CHA of *c*-octane. When *c*-octene accumulates, it serves as a trap for $Rh_2(ttp)_2$ **6** and therefore stops the CCA.

Rh(ttp)H as Intermediate in CCA? To investigate whether Rh(ttp)H is the intermediate for CCA, Rh(ttp)H **4** was reacted with *c*-octane. Rh(ttp)H indeed reacted with *c*-octane at 120 °C

DOI: 10.1021/acs.organomet.5b00183
Organometallics XXXX, XXX, XXX−XXX

in 15 h to give Rh(ttp)(*n*-octyl) **3** selectively, though in only 21% yield, and was also recovered in 73% yield (eq 2).

$$\underset{73\%\text{ recovered}}{\text{Rh(ttp)H}} + \textit{c}\text{-octane} \xrightarrow[15\text{ h, }N_2]{120\ ^\circ\text{C}} \underset{\mathbf{3}\ 21\%}{\text{Rh(ttp)}(\textit{n}\text{-octyl})} \quad (2)$$

Prolonged heating of Rh(ttp)H in *c*-octane over 12 d yielded Rh(ttp)(*n*-octyl) and $Rh_2(ttp)_2$ in 94% and 2% yields, respectively (eq 3). As Rh(ttp)H underwent slow dehydrogen-

$$\text{Rh(ttp)H} + \textit{c}\text{-octane} \xrightarrow[12\text{ d, }N_2]{120\ ^\circ\text{C}} \underset{\mathbf{3}\ 94\%}{\text{Rh(ttp)}(\textit{n}\text{-octyl})} + \underset{\mathbf{6}\ 2\%}{\text{Rh}_2(\text{ttp})_2} \quad (3)$$

ative dimerization to give 6% yield of $Rh_2(ttp)_2$ at 120 °C in 1 day (eq 4), similar to the report by Wayland and co-workers,[18] the small amount of $Rh_2(ttp)_2$ formed may facilitate the 1,2-addition of Rh(ttp)H into *c*-octane (see the discussion below).

$$\underset{91\%\text{ recovered}}{2\text{Rh(ttp)H}} \xrightarrow[120\ ^\circ\text{C, 1 d}]{\text{benzene-}d_6} \underset{\mathbf{6}\ 6\%}{\text{Rh}_2(\text{ttp})_2} + \text{"}H_2\text{"} \quad (4)$$

It is intuitively tempting to suggest that Rh(ttp)H undergoes a 1,2-insertion into the CC bond of *c*-octane by σ-bond metathesis (Scheme 2).[19] However, the requirement of a 12 d

Scheme 2. 4-Centered Transition State via σ-Bond Metathesis Can Be Excluded

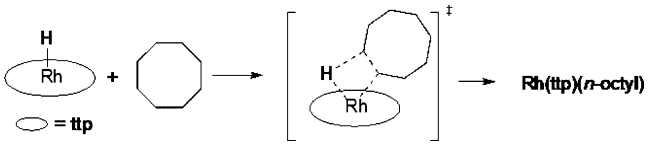

reaction time rules out the fact that Rh(ttp)H is a direct intermediate involved in the CC bond activation reaction. The fairly crowded 4-centered transition state in the same size of Rh porphyrin is geometrically not very attractive. Indeed, the reaction mixture of 1 equiv of PPh_3, Rh(ttp)H, and *c*-octane upon heating at 120 °C for 1.5 d gave quantitative Rh(ttp)H(PPh_3) but no Rh(ttp) *n*-octyl **3** (eq 5). Rh(ttp)H(PPh_3) did not undergo any dimerization, and therefore no Ph_3P was ligated to $Rh_2(ttp)_2$. No CCA of *c*-octane with Rh(ttp)H alone occurs at a fast enough rate.

$$\underset{\mathbf{4}}{\text{Rh(ttp)H}} + PPh_3 + \textit{c}\text{-octane} \xrightarrow[1.5\text{ d, }N_2]{120\ ^\circ\text{C}} \underset{\text{quantitative}}{\text{Rh(ttp)H}(PPh_3)} \quad (5)$$

$Rh_2(ttp)_2$ as an Intermediate in CCA? We next examined whether $Rh_2(ttp)_2$ **6** is a possible intermediate. $Rh_2(ttp)_2$ **6** reacted with *c*-octane at 120 °C for 15 h to give Rh(ttp)(*c*-octyl) **2**, Rh(ttp)(*n*-octyl) **3**, and Rh(ttp)H **4** in 41%, 4%, and 46% yields, respectively (eq 6) with a very low yield of CCA

$$\underset{\mathbf{6}}{\text{Rh}_2(\text{ttp})_2} + \textit{c}\text{-octane} \xrightarrow[15\text{ h, }N_2]{120\ ^\circ\text{C}} \underset{\mathbf{2}\ 41\%}{\text{Rh(ttp)}(\textit{c}\text{-octyl})} + \underset{\mathbf{3}\ 4\%}{\text{Rh(ttp)}(\textit{n}\text{-octyl})} + \underset{\mathbf{4}\ 46\%}{\text{Rh(ttp)H}} \quad (6)$$

product **3** and is therefore not a major intermediate. Therefore, both Rh(ttp)H **4** and $Rh_2(ttp)_2$ **6** separately gave low yielding reactions and are likely only minor reaction intermediates by themselves. We therefore investigated the synergistic effect of both Rh(ttp)H **4** and $Rh_2(ttp)_2$ **6** to give Rh(ttp)(*n*-octyl) **3**.

Proposed Mechanism of Rh^{II}(ttp)-Catalyzed 1,2-Insertion of Rh(ttp)H into the Carbon−Carbon Bond of *c*-Octane. We anticipated that the metalloradical Rh^{II}(ttp) **7**/$Rh_2(ttp)_2$ may act as a catalyst to facilitate the 1,2-addition of *c*-octane with Rh(ttp). Indeed, Halpern reported in the elegant mechanistic studies that Rh^{II}(oep) catalyzes (oep = octylethylporphyrin dianion) the 1,2-addition of styrene to give Rh(oep)CH_2CH_2Ph[20] Rh^{II}(oep), which forms from homolysis of the weak Rh−Rh bond in $Rh_2(oep)_2$,[18] inserts into the C=C bond of styrene to give a Rh(oep)CH_2C·HPh benzylic carbon-centered radical, which is also a reversible reaction. The Rh(oep)CH_2CHPh radical then abstracts a hydrogen atom from Rh(oep)H to yield the 1,2-addition product Rh(oep)-CH_2CH_2Ph and regenerates Rh^{II}(oep). Thus, it is a Rh^{II}(ttp)-catalyzed 1,2-insertion of Rh(ttp)H into the carbon−carbon bond of styrene.

We thus recognized the similarity and anticipated that the CCA of *c*-octane, being a 1,2-addition reaction, can also be catalyzed by Rh^{II}(ttp) **7** (Scheme 3). $Rh_2(ttp)_2$ **5** formed from

Scheme 3. Proposed Rh(ttp)-Catalyzed 1,2-Insertion of Rh(ttp)H into the Carbon−Carbon Bond of *c*-Octane

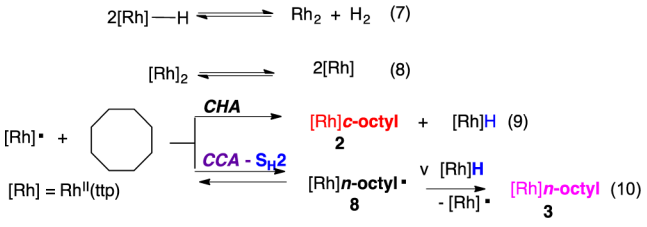

the thermolysis of Rh(ttp)H (eq 7, Scheme 3), initially undergoes homolysis to give Rh^{II}(ttp) (eq 8 in ref).[18] Rh^{II}(ttp) **7** then reacts with *c*-octane in parallel CHA (eq 9, Scheme 3) and CCA (eq 10, Scheme 3). For the CCA pathway, Rh^{II}(ttp) can cleave the C−C bond of *c*-octane to generate the alkyl radical **8** by a bimolecular homolytic substitution (S_H2)-like process[22] (eq 10, Scheme 3) which can also reverse rapidly.[20] Compound **8** can then abstract a hydrogen atom from the weak (ttp)Rh-H bond (~60 kcal mol^{-1}),[21] serving as an alkyl radical trap to form a strong alkyl C−H bond[21b] to provide the driving force of the reaction (eq 10, Scheme 3).

The branching of CHA and CCA is reasoned to be strongly dependent on the concentration of $Rh_2(ttp)_2$. Rh^{II}(por) has been shown to undergo CHA with alkane to give Rh(por)R and Rh(por)H with a termolecular rate law (eq 9, Scheme 3).[8] The proposed CCA should, however, follow first order kinetics in Rh^{II}(ttp) or half order kinetics in $Rh_2(ttp)_2$, thus requiring much lower Rh^{II}(ttp) concentrations. At the same time, a large excess concentration of Rh(ttp)H facilitates trapping of the carbon-centered radical **8** to give **3** and to regenerate Rh^{II}(ttp) **7**. In this mechanism, $Rh_2(ttp)_2$ is the precatalyst or more precisely Rh^{II}(ttp) is the catalyst, but the reaction requires the presence of Rh(ttp)H in excess. To validate this mechanism, and to develop a selective CCA process, we conducted a series of experiments for the reaction with *c*-octane by increasing the concentration ratio of Rh(ttp)H/$Rh_2(ttp)_2$ for more efficient trapping.

Synergetic Effect of Rh(ttp)H/$Rh_2(ttp)_2$ in CCA of *c*-Octane. Indeed, mixtures of Rh(ttp)H and $Rh_2(ttp)_2$ were much more efficient reagents, and the use of the combination of both enhanced the total yields to up to 79% (Table 5, entries 2−4 vs 1). The selectivity toward CCA was further enhanced

DOI: 10.1021/acs.organomet.5b00183
Organometallics XXXX, XXX, XXX−XXX

Table 5. Rh^{II}(ttp)-Catalyzed CCA of *c*-Octane with Rh(ttp)H

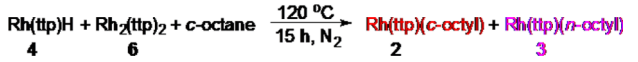

entry[a]	Rh(ttp)H/Rh_2(ttp)$_2$ 4:6	yield **2** (%)	yield **3** (%)	total yield (%)
1[b]	01:0	00	21	21
2	02:1	60	18	78
3	05:1	53	26	79
4	10:1	00	73	73

[a]The results are the average of at least duplicate measurements. [b]73% Rh(ttp)H recovered.

by an increase of the Rh(ttp)H/Rh_2(ttp)$_2$ ratio. The CCA of *c*-octane with the mixture of Rh(ttp)H/Rh_2(ttp)$_2$ in 2:1 ratio gave Rh(ttp)(*c*-octyl) **2** and Rh(ttp)(*n*-octyl) **3** in 60% and 18% yields, respectively (Table 5, entry 2). When the Rh(ttp)H/Rh_2(ttp)$_2$ ratio increased to 5:1, the yield of Rh(ttp)(*n*-octyl) **3** increased to 26% yield but that of Rh(ttp)(*c*-octyl) **2** decreased to 53% yield (entry 3). We were glad to observe that Rh(ttp)(*n*-octyl) **3** was selectively obtained in 73% yield from the reaction with the 10:1 ratio of Rh(ttp)H/Rh_2(ttp)$_2$ (entry 4). The elimination of the CHA channel (eq 9, Scheme 3) by a low concentration of Rh_2(ttp)$_2$ **6** and efficient trapping of **8** by a higher concentration of Rh(ttp)H were achieved. The selective aliphatic CCA of *c*-octane was thus realized successfully, and the results confirm the proposed Rh^{II}(ttp)-catalyzed 1,2-addition of Rh(ttp)H over the C−C bond of *c*-octane.

Influence of Porphyrin Sterics on CCA. To find out the steric sensitivity of CCA toward porphyrin structure, we further examined the reaction of *c*-octane with the analogous but sterically more hindered Rh(tmp) complexes (tmp = 5,10,15,20-tetramesitylporphyrinato dianion).[8] Rh(tmp)Cl **10** reacted with *c*-octane (20 equiv) and K_2CO_3 in benzene-d_6 at 120 °C in 3d to give Rh(tmp)H, Rh(tmp), and *c*-octene in 51%, 46%, and 28%, respectively without any CCA product (eq 11). When the mixture of Rh(tmp)H **11** and Rh^{II}(tmp) **12**

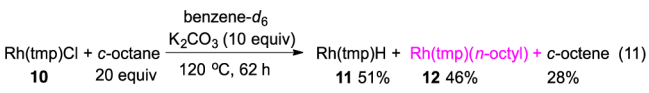

(10:1) was reacted with *c*-octane at 120 °C for 15 h, no reaction occurred, and 90% yield of Rh(tmp)H **11** was recovered (eq 12). Rh^{II}(tmp) **12** alone only underwent CHA with *c*-octane to give Rh(tmp)H **11** and *c*-octene in 86% and 40% yields, respectively (eq 13).

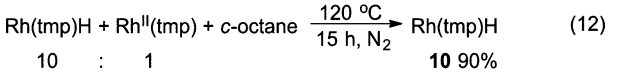

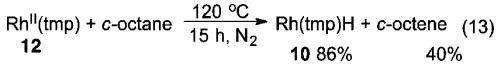

The formation of *c*-octene likely results from the bimetalloradical CHA to give Rh(tmp)(*c*-octyl) **13**, which then rapidly undergoes facile *β*-hydride elimination to give *c*-octene and Rh(tmp)H **7**. The nearly 1:2 ratio of Rh(tmp)H to *c*-octene further supports the occurrence of this process. The *β*-hydride elimination of **13** is sterically enhanced by the unfavorable steric interactions of the methyl groups at the 2,6 positions of mesityl groups in Rh(tmp) with the c-octyl group resulting in a slight weakening of the Rh-*c*-octyl bond (Scheme 4).[23] Indeed, the attempted synthesis of Rh(tmp)(*c*-octyl) **13**

Scheme 4. Formation of Rh(tmp)H from CHA of Rh^{II}(tmp) and *c*-Octane

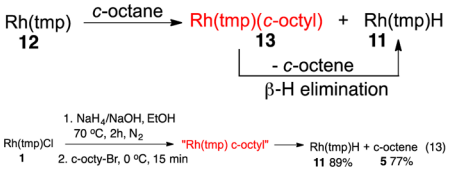

by the reductive alkylation ($NaBH_4$/*c*-octyl bromide) at a lower temperature of 50 °C gave Rh(tmp)H **9** and *c*-octene in 89 and 77% yields, respectively, showing the highly labile nature of Rh(tmp)-*c*-octyl **13** compared to Rh(ttp) *c*-octyl **2** (eq 1).

DFT Theoretical Calculations of the Proposed CCA Step. To gain further understanding of the metalloradical CCA step, DFT calculations were performed. Initial comparative screening of different reaction pathways was performed at the DFT-D3, b3-lyp, def2-TZVP levels using small atom Rh(por) models of the actual Rh(tpp) species containing nonfunctionalized porphyrin rings without *meso*-phenyl substituents.

All attempts to find a transition state corresponding to the *σ*-bond metathesis 4-centered transition state described in Scheme 2 were unsuccessful and led to the transition states $\mathbf{TS_A}$ or $\mathbf{TS_B}$ corresponding to pathways A and B in Scheme 5. These pathways correspond to hypothetical reactions in which (por)Rh-octyl is formed directly from (por)Rh−H and the *c*-octane reagent. In closed-shell singlet pathway A, simultaneous heterolysis of the C−C bond of *c*-octane is accompanied by proton transfer from the Rh-hydride moiety of (por)Rh−H to the resulting negatively charged carbon atom formed from *c*-octane in $\mathbf{TS_A}$. The transition state leads to subsequent proton transfer from the beta-position of the "cationic" carbon to rhodium, producing 1-octene with regeneration of (por)Rh−H. Subsequent insertion of 1-octene into the Rh−H bond of (por)Rh−H could produce (por)Rh-octyl, but the transition state of this hypothetical step was not investigated in view of the very high barrier of the preceding transition state $\mathbf{TS_A}$. While interesting from a fundamental perspective, the high transition state barrier of $\mathbf{TS_A}$ makes pathway A rather unrealistic. The same holds for pathway B, which proceeds at the open-shell singlet (singlet biradical) surface employing the broken-symmetry approach. This pathway involves C−C bond homolysis of *c*-octane associated with simultaneous hydrogen-atom transfer from (por)Rh−H to the (developing) ·C_8H_{16}· diradical, thus producing (por)Rh^{II} and the 1-octyl radical ·C_8H_{17}. Subsequent formation of (por)Rh-octyl is virtually barrierless and only requires a proper orientation of the Rh^{II}(por) and 1-octyl radical ·C_8H_{17} reagents to allow Rh−C bond formation. Again, pathway B is fundamentally interesting but has a very high transition state barrier $\mathbf{TS_B}$, making this pathway rather unrealistic in view of the experimental observations.

In marked contrast to pathways A and B, the transition state barrier TS_C of pathway C involving a Rh^{II}(por) metalloradical catalyzed reaction between (por)Rh−H and *c*-octane is much lower, and hence, pathway C is a much more realistic scenario, in good agreement with the experimental data (Scheme 5). This pathway involves homolytic activation of the C−C bond of *c*-octane by the Rh^{II}(por) metalloradical producing a

DOI: 10.1021/acs.organomet.5b00183
Organometallics XXXX, XXX, XXX−XXX

Scheme 5. Comparison of DFT Calculated Free Energies ($\Delta G_{298\ K}$ in kcal mol^{-1}) of Different Pathways Leading to the Formation of (por)Rh-octyl from (por)Rh-H and *c*-Octane (DFT-D3, b3-lyp, and def2-TZVP)

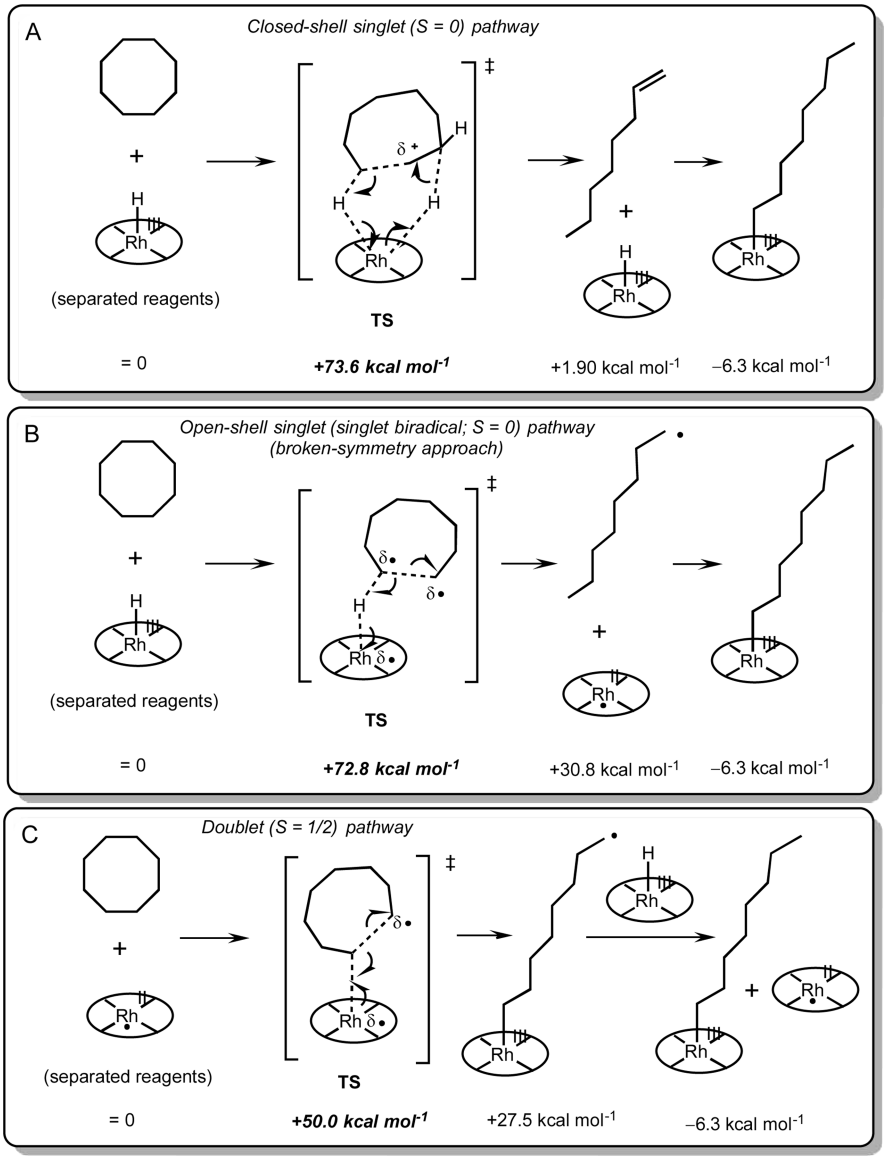

terminal octyl-radical species (por)Rh−C_8H_{16}·, which subsequently abstracts a hydrogen atom from (por)Rh−H to regenerate the (por)Rh^{II} metalloradical "catalyst" with the formation of the (por)Rh-octyl product.

Pathway C was further explored in more detail using the full atom Rh(tpp) models. We argued that the full atom models might lead to lower barriers in view of stronger (VdW) dispersion interactions between *c*-octane and the Rh(tpp) species. As such, we examined the hypothesized CCA reaction between Rh^{II}(tpp) and *c*-octane, followed by reaction of the Rh(tpp)octyl radical complex **III** with Rh(tpp)(H) to form Rh(tpp)octyl and to regenerate Rh^{II}(tpp) (see Scheme 6). We employed both the BP86 and the b3-lyp functional to examine the details of pathway C. The def2-TZVP basis set and Grimme's D3-DFT dispersion corrections were used in both cases. For the b3-lyp pathways, additional cosmo dielectric solvent corrections (ε = 2.27 corresponding to benzene) were included. The (free) energies associated with the reaction sequence depicted in Scheme 6 are listed in Table 6.

The DFT calculated pathway (Scheme 6) is in qualitative agreement with the proposed mechanism (Scheme 3). The first steps from **I** to **III** are endothermic and endergonic. This agrees with the experimental requirement to heat to drive the reaction. The subsequent reaction between the Rh(tpp)octyl radical complex **III** with Rh(tpp)(H) to form Rh(tpp)octyl and Rh^{II}(tpp) is exothermic and exergonic, and provides the driving force of the overall reaction. We were unable to find a transition state for this last step, likely because the barrier is too low with a flat reaction profile. The transition state of the first reaction step (from **II** via **TS** to **III**) involves a metallo-radical induced S_H2-type homolysis of one of the C−C bonds of *c*-octane. In this CCA pathway, the Rh^{II} metallo-radical traps one of the two carbon radicals produced in this process in concert with C−C bond homolysis (Figure 1).

Despite stronger attractive dispersion (VdW) forces between Rh(tpp) and *c*-octane, the $\mathbf{TS}_C$ transition barrier is still sizable at the b3-lyp level (Table 1). However, it should be recalled at this point that the experimental reaction requires prolonged (15 h) heating to 120 °C to reach completion, and hence the

DOI: 10.1021/acs.organomet.5b00183
Organometallics XXXX, XXX, XXX−XXX

Scheme 6. DFT Calculated Metallo-Radical Catalyzed Reaction between *c*-Octane and (por)Rh-H (Pathway C) Including Selected Bond Lengths[a]

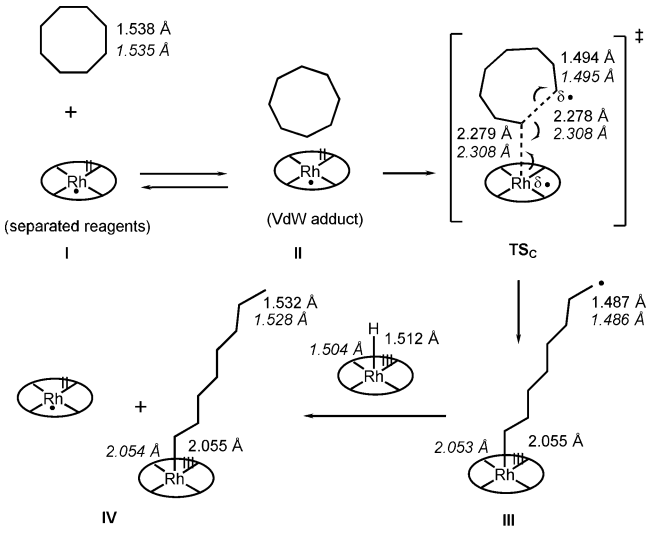

[a]DFT-D3, BP86, def2-TZVP, and DFT-D3, b3-lyp, def2-TZVP, and cosmo ε = 2.27.

Table 6. DFT Calculated Energies Associated with the Computed Reaction Pathway Depicted in Scheme 6[a]

	ΔE_{ZPE} (kcal mol^{-1}) BP86 b3-lyp	$\Delta G^{\circ}_{(298\ K)}$ (kcal mol^{-1}) BP86 b3-lyp	ΔH° (kcal mol^{-1}) BP86 b3-lyp	ΔS° (cal mol^{-1} K^{-1}) BP86 b3-lyp
I	= 0	= 0	= 0	= 0
II	−15.9	−8.3	−15.7	−24.8
	−10.2	−5.5	−9.5	−13.3
TS	+20.0	+28.5	+20.1	−28.0
	+34.5	+42.0	+34.9	−24.4
III	+9.2	+13.7	+10.8	−9.7
	+17.0	+22.6	+18.1	−14.9
IV	−17.8	−17.8	−17.0	+2.6
	−16.0	−17.9	−14.7	+10.6

[a]DFT-D3, BP86, def2-TZVP, and DFT-D3; b3-lyp, def2-TZVP, and cosmo ε = 2.27.

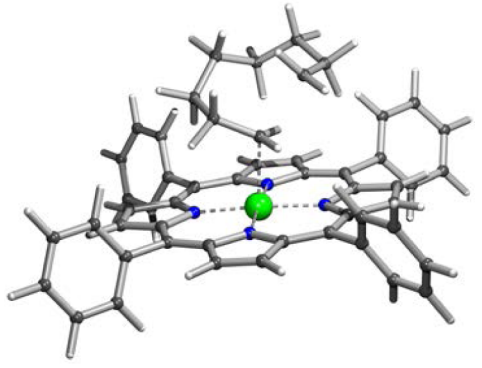

Figure 1. Structure of transition state TS representing Rh^{II}-mediated S_H2-type CCA of *c*-octane (b3-lyp, def2-TZVP).

experimental barrier is also high (estimated at ∼30−35 kcal mol^{-1}). The barrier (from **II** to **TS$_C$**) calculated at the BP86, def2-TZVP level ($\Delta G^{\ddagger}$ = 36.8 kcal mol^{-1}; $\Delta H^{\ddagger}$ = 35.8 kcal mol^{-1}) is lower and in reasonable agreement with the experimental estimate. The barrier calculated at the b3-lyp, def2-TZVP seems to be overestimated by several kcal mol^{-1} (which is not uncommon in DFT studies[24]).

Conclusions. We have discovered the Rh^{II}(ttp)-catalyzed 1,2-insertion of Rh(ttp)H into the carbon−carbon bond of *c*-octane, which selectively produces Rh(ttp)-*n*-octyl in high yield. The Rh^{II}(ttp) metallo-radical attacks the C−C bond of *c*-octane, likely via an S_H2 process. DFT theoretical calculations support this mechanistic proposal. This represents a unique metalloradical carbon−carbon activation process. Further studies are being continued to develop catalytic C−C bond functionalization.

EXPERIMENTAL AND COMPUTATIONAL DETAILS

Reaction of *c*-Octane with Rh(ttp)Cl. Rh(ttp)Cl **1** (20.6 mg, 0.026 mmol) was added in *c*-octane (3.0 mL). The red reaction mixture was degassed for three freeze−thaw−pump cycles, purged with N_2, and heated at 120 °C under N_2 for 48 h. Excess *c*-octane was removed by vacuum distillation. The residue was purified by column chromatography on silica gel eluting with a solvent mixture of hexane/CH_2Cl_2 (1:1). Red solid, Rh(ttp)(*c*-octyl) **2** (1.0 mg, 0.0011 mmol, 5%), and Rh(ttp)(*n*-octyl) **3** (1.9 mg, 0.0021 mmol, 8%) were collected and further recrystallized from CH_2Cl_2/MeOH. The product ratio was calculated by ^{1}H NMR integration. Rh(ttp)Cl was recovered (14.8 mg) after column chromatography. Characterization of Rh(ttp)(*c*-octyl) **2**: R_f = 0.84 (hexane/CH_2Cl_2 = 1:1). ^{1}H NMR (C_6D_6, 400 MHz) δ −4.25 (m, 2), −3.66 (m, 3 H), −1.13 (m, 4 H), −0.32 (m, 2 H), 0.90 (m, 4 H), 2.41 (s, 12 H, *p*-methyl), 7.30 (d, 4 H, J = 7.3 Hz, *m*-phenyl), 7.33 (d, 4 H, J = 7.2 Hz, *m*′-phenyl), 8.18 (d, 4 H, J = 7.7 Hz, *o*′-phenyl), 8.97 (s, 8 H, pyrrole). ^{13}C NMR ($CDCl_3$, 75 MHz) δ 21.70, 22.54, 25.23, 25.85, 30.40, 40.62 (d, $^1J_{Rh-C}$ = 26.4 Hz), 122.86, 127.42, 127.54, 131.48, 133.62, 134.25, 137.22, 139.52, 143.52. HRMS calcd. for $(C_{56}H_{51}N_4Rh+H)^+$: m/z 883.3242. Found: m/z 883.3214. Characterization of Rh(ttp)(*n*-octyl) **2**: R_f = 0.84 (hexane/CH_2Cl_2 = 1:1). ^{1}H NMR (C_6D_6, 400 MHz) δ −4.55 (td, 2 H, J = 2.8, 8.7 Hz), −4.11 (qu, 2 H, J = 8.2 Hz), −1.55 (qu, 2 H, J = 7.8 Hz), −0.50 (qu, 2 H, J = 8.0 Hz), 0.02 (qu, 2 H, J = 7.5 Hz), 0.44 (qu, 2 H, J = 7.4 Hz), 0.59 (t, 3 H, J = 7.2 Hz), 0.80 (qu, 2 H, J = 7.6 Hz), 2.41 (s, 12 H, *p*-methyl), 7.27 (d, 4 H, J = 8.1 Hz, *m*-phenyl), 7.35 (d, 4 H, J = 6.4 Hz, *m*′-phenyl), 8.12 (dd, 4 H, J = 1.7, 7.6 Hz, *o*-phenyl), 8.22 (dd, 4 H, J = 1.6, 7.6 Hz, *o*′-phenyl), 8.99 (s, 8 H, pyrrole). ^{13}C NMR ($CDCl_3$, 100 MHz) δ 14.00, 15.69 (d, $^1J_{Rh-C}$ = 26.8 Hz), 21.68, 22.41, 26.28, 27.04, 27.52, 27.96, 31.31, 122.49, 127.43, 127.51, 131.47, 133.78, 134.09, 137.23, 139.48, 143.35. HRMS calcd. for $(C_{56}H_{53}N_4Rh)^+$: m/z 884.3320. Found: m/z 884.3336.

Reaction of *c*-Octane and Rh(ttp)Cl with Potassium Hydroxide. Rh(ttp)Cl (20.4 mg, 0.025 mmol) and potassium hydroxide (14.2 mg, 0.254 mmol) was added in *c*-octane (3.0 mL). The red reaction mixture was degassed for three freeze−thaw−pump cycles, purged with N_2 and heated at 120 °C under N_2 for 7.5 h. Excess *c*-octane was removed by vacuum distillation. The red residue was added with benzene-d_6 (500 μL) under N_2 for ^{1}H NMR spectroscopy, and the NMR yield of Rh(ttp)H (62%) was estimated. The crude mixture was then extracted with CH_2Cl_2/H_2O. The organic layer was collected, dried, and evaporated to dryness, and the residue was purified by column chromatography on silica gel eluting with a solvent mixture of hexane/CH_2Cl_2 (1:1). Red solids, Rh(ttp)(*c*-octyl) **2** (1.3 mg, 0.0015 mmol, 6%), and Rh(ttp)(*n*-octyl) **3** (5.6 mg, 0.0063 mmol, 25%) were collected.

Reaction of *c*-Octane and Rh(ttp)Cl with Potassium Carbonate. Rh(ttp)Cl (20.4 mg, 0.025 mmol) and anhydrous potassium carbonate (34.9 mg, 0.252 mmol) were added in *c*-octane (3.0 mL). The red reaction mixture was degassed for three freeze−thaw−pump cycles, purged with N_2, and heated at 120 °C under N_2 for 7.5 h. Excess *c*-octane was removed by vacuum distillation. The red residue was added with benzene-d_6 (500 μL) under N_2 for ^{1}H NMR spectroscopy, and the NMR yield of Rh(ttp)H (58%) was estimated. The crude mixture was then extracted with CH_2Cl_2/H_2O. The organic layer was collected, dried, and evaporated to dryness, and the residue

DOI: 10.1021/acs.organomet.5b00183
Organometallics XXXX, XXX, XXX−XXX

was purified by column chromatography on silica gel eluting with a solvent mixture of hexane/CH_2Cl_2 (1:1). Red solids, Rh(ttp)(*n*-octyl) **3** (7.5 mg, 0.0085 mmol, 33%), were collected.

Independent Synthesis of Rh(ttp)(*c*-octyl) 2.[6] A suspension of Rh(ttp)Cl (100 mg, 0.11 mmol) in EtOH (50 mL) and a solution of $NaBH_4$ (17 mg, 0.45 mmol) in aq. NaOH (0.1 M, 2 mL) were purged with N_2 for 15 min separately. The solution of $NaBH_4$ was added slowly to the suspension of Rh(ttp)Cl via a cannula. The mixture was heated at 50 °C under N_2 for 1 h. The solution was then cooled to 30 °C under N_2 and *c*-octyl bromide (23 mg, 1.20 mmol) was added. A reddish orange suspension was formed. After stirring at room temperature for another 15 min under N_2, the reaction mixture was worked up by extraction with CH_2Cl_2/H_2O. The combined organic extract was dried ($MgSO_4$), filtered, and rotatory evaporated. The reddish orange residue was purified by column chromatography over silica gel (250−400 mesh) using a solvent mixture of hexane/CH_2Cl_2 (1:1) as the eluent. The major orange fraction was collected and gave a reddish orange solid of Rh(ttp)(*c*-octyl) **2** (94.1 mg, 0.11 mmol, 86%) as the product after rotary evaporation.

Independent Synthesis of Rh(ttp)(*n*-octyl) 3.[6] A suspension of Rh(ttp)Cl (100 mg, 0.11 mmol) in EtOH (50 mL) and a solution of $NaBH_4$ (17 mg, 0.45 mmol) in aq. NaOH (0.1 M, 2 mL) were purged with N_2 for 15 min separately. The solution of $NaBH_4$ was added slowly to the suspension of Rh(ttp)Cl via a cannula. The mixture was heated at 50 °C under N_2 for 1 h. The solution was then cooled to 30 °C under N_2, and *n*-octyl bromide (23 mg, 1.20 mmol) was added. A reddish orange suspension was formed. After stirring at room temperature for another 15 min under N_2, the reaction mixture was worked up by extraction with CH_2Cl_2/H_2O. The combined organic extract was dried ($MgSO_4$), filtered, and rotatory evaporated. The reddish orange residue was purified by column chromatography over silica gel (250−400 mesh) using a solvent mixture of hexane/CH_2Cl_2 (1:1) as the eluent. The major orange fraction was collected and gave a reddish orange solid of Rh(ttp)(*n*-octyl) **3** (96.5 mg, 0.11 mmol, 88%) as the product after rotary evaporation.

Thermal Stability of Rh(ttp)(*c*-octyl) in Benzene-d_6. Rh(ttp)(*c*-octyl) **2** (3.9 mg, 0.0044 mmol) was added into benzene-d_6 (500 μL) in a NMR tube. The red solution was degassed for three freeze−thaw−pump cycles, and the NMR tube was flame-sealed under vacuum. It was heated at 120 °C in the dark. It was monitored with ^{1}H NMR spectroscopy at particular time intervals, and the NMR yields were taken.

Stability of Rh(ttp)(*c*-octyl) with Potassium Carbonate in Benzene-d_6. Rh(ttp)(*c*-octyl) **2** (3.9 mg, 0.0044 mmol) and potassium carbonate (6.0 mg, 0.044 mmol) were added into benzene-d_6 (500 μL) in a NMR tube. The red solution was degassed for three freeze−thaw−pump cycles, and the NMR tube was flame-sealed under vacuum. It was heated at 120 °C in the dark. It was monitored with ^{1}H NMR spectroscopy at particular time intervals, and the NMR yields were taken.

Reaction of Rh(ttp)Cl and *c*-Octane with Potassium Carbonate in Benzene-d_6. Rh(ttp)Cl (3.5 mg, 0.0043 mmol), *c*-octane (11 μL, 0.087 mmol), and potassium carbonate (5.9 mg, 0.0427 mmol) were added into benzene-d_6 (500 μL) in a NMR tube. The red mixture was degassed for three freeze−thaw−pump cycles, and the NMR tube was flame-sealed under vacuum. It was heated at 120 °C in the dark. It was monitored with ^{1}H NMR spectroscopy at particular time intervals, and the NMR yields were taken.

Reaction of *c*-Octane with Rh(ttp)H. Rh(ttp)H (9.6 mg, 0.012 mmol) was added in *c*-octane (1.5 mL). The red reaction mixture was degassed for three freeze−thaw−pump cycles, purged with N_2, and heated at 120 °C under N_2 for 15 h. Excess *c*-octane was removed by vacuum distillation. The residue was added with benzene-d_6 (500 μL) under N_2 protection for ^{1}H NMR spectroscopy, and the recovered yield of Rh(ttp)H (73%) was estimated. The residue was purified by column chromatography on silica gel eluting with a solvent mixture of hexane/CH_2Cl_2 (1:1). Red solid, Rh(ttp)(*n*-octyl) **3** (2.3 mg, 0.0026 mmol, 21%), was collected and was further recrystallized from CH_2Cl_2/MeOH.

Reaction of *c*-Octane with Rh(ttp)H and PPh_3. Rh(ttp)H (9.6 mg, 0.012 mmol) and PPh3 (3.2 mg, 0.012 mmol) were added in *c*-octane (1.5 mL). The red reaction mixture was degassed for three freeze−thaw−pump cycles, purged with N_2, and heated at 120 °C under N_2 for 15 h. Excess *c*-octane was removed by vacuum distillation. The residue was added with benzene-d_6 (500 μL) under N_2 protection for ^{1}H NMR spectroscopy. Rh(ttp)H(PPh_3) was obtained in quantitative NMR yield. ^{1}H NMR (C_6D_6, 400 MHz) δ −33.42 (b, 1 H), 2.39 (s, 12 H, *p*-methyl), 4.16 (t, 2 H, J = 9.2 Hz), 6.28 (td, 2 H, J = 2.4, 7.6 Hz, *m*-phenyl), 6.52 (t, 1 H, J = 6.8 Hz), 7.35 (d, 4 H, J = 7.2 Hz, *m*′-phenyl), 7.84 (d, 4 H, J = 7.6 Hz, *o*-phenyl), 7.89 (d, 4 H, J = 7.6 Hz, *o*′-phenyl), 8.98 (s, 8 H, pyrrole).

Thermal Dehydrogenative Dimerization of Rh(ttp)H. Rh(ttp)H (3.2 mg, 0.0041 mmol) was added in benzene-d_6 (500 μL). The red reaction mixture was degassed for three freeze−thaw−pump cycles, and the NMR tube was flame-sealed under vacuum. It was heated at 120 °C in the dark. It was monitored with ^{1}H NMR spectroscopy at particular time intervals, and the NMR yields of $Rh_2(ttp)_2$ **6** were taken. The H_2 concentration in solution was too low to be detected.

Reaction of *c*-Octane with $Rh_2(ttp)_2$ 6. $Rh_2(ttp)_2$ (9.6 mg, 0.012 mmol) was added in *c*-octane (1.5 mL). The red reaction mixture was degassed for three freeze−thaw−pump cycles, purged with N_2, and heated at 120 °C under N_2 for 15 h. Excess *c*-octane was removed by vacuum distillation. The red residue was added with benzene-d_6 (500 μL) under N_2 protection for ^{1}H NMR spectroscopy, and the yield of Rh(ttp)H (46%) was estimated. The residue was purified by column chromatography on silica gel eluting with a solvent mixture of hexane/CH_2Cl_2 (1:1). Red solids, Rh(ttp)(*c*-octyl) **2** (4.5 mg, 0.0051 mmol, 41%) and Rh(ttp)(*n*-octyl) **3** (0.4 mg, 0.00045 mmol, 4%), were collected, and the product ratio was calculated by ^{1}H NMR integration.

Reaction of *c*-Octane with a 2:1 Mixture of Rh(ttp)H and $Rh_2(ttp)_2$. Rh(ttp)H (9.6 mg, 0.012 mmol) and $Rh_2(ttp)_2$ (4.8 mg, 0.0031 mmol) were added to *c*-octane (1.5 mL). The red reaction mixture was degassed for three freeze−thaw−pump cycles, purged with N_2, and heated at 120 °C under N_2 for 15 h. Excess *c*-octane was removed by vacuum distillation. The residue was purified by column chromatography on silica gel eluting with a solvent mixture of hexane/CH_2Cl_2 (1:1). Red solids, Rh(ttp)(*c*-octyl) **2** (9.8 mg, 0.011 mmol, 60%) and Rh(ttp)(*n*-octyl) **3** (3.0 mg, 0.0034 mmol, 18%), were collected, and the product ratio was calculated by ^{1}H NMR integration.

Reaction of *c*-Octane with a 5:1 Mixture of Rh(ttp)H and $Rh_2(ttp)_2$. Rh(ttp)H (9.6 mg, 0.012 mmol) and $Rh_2(ttp)_2$ (1.9 mg, 0.0012 mmol) were added to *c*-octane (1.5 mL). The red reaction mixture was degassed for three freeze−thaw−pump cycles, purged with N_2, and heated at 120 °C under N_2 for 15 h. Excess *c*-octane was removed by vacuum distillation. The residue was purified by column chromatography on silica gel eluting with a solvent mixture of hexane/CH_2Cl_2 (1:1). Red solids, Rh(ttp)(*c*-octyl) **2** (6.9 mg, 0.0078 mmol, 53%) and Rh(ttp)(*n*-octyl) **3** (3.4 mg, 0.0038 mmol, 26%), were collected, and the product ratio was calculated by ^{1}H NMR integration.

Reaction of *c*-Octane with a 10:1 Mixture of Rh(ttp)H and $Rh_2(ttp)_2$. Rh(ttp)H (9.6 mg, 0.012 mmol) and $Rh_2(ttp)_2$ (1.0 mg, 0.00065 mmol) were added to *c*-octane (1.5 mL). The red reaction mixture was degassed for three freeze−thaw−pump cycles, purged with N_2, and heated at 120 °C under N_2 for 15 h. Excess *c*-octane was removed by vacuum distillation. The residue was purified by column chromatography on silica gel eluting with a solvent mixture of hexane/CH_2Cl_2 (1:1). Red solid, Rh(ttp)(*n*-octyl) **3** (8.9 mg, 0.010 mmol, 73%) was collected and was further recrystallized from CH_2Cl_2/MeOH.

Reaction of Rh(tmp)Cl 10 and *c*-Octane with Potassium Carbonate in Benzene-d_6. Rh(tmp)Cl[9,10] (4.0 mg, 0.0043 mmol), *c*-octane (11 μL, 0.087 mmol), and potassium carbonate (5.8 mg, 0.0420 mmol) were added into benzene-d_6 (500 μL) in a NMR tube. The red mixture was degassed for three freeze−thaw−pump cycles, and the NMR tube was flame-sealed under vacuum. It was heated at

DOI: 10.1021/acs.organomet.5b00183
Organometallics XXXX, XXX, XXX−XXX

120 °C in the dark. It was monitored with ^{1}H NMR spectroscopy at particular time intervals, and the NMR yields were taken. Rh(tmp)H, Rh^{II}(tmp), and *c*-octene were in 51%, 46%, and 28% yields, respectively at 120 °C in 3 d.

Reaction of *c*-Octane with a 10:1 Mixture of Rh(tmp)H 11 and Rh^{II}(tmp) 12. Rh(tmp)H[8] (10.6 mg, 0.012 mmol) and Rh^{II}(tmp)[8] (1.1 mg, 0.0012 mmol) were added to *c*-octane (1.5 mL). The red reaction mixture was degassed for three freeze−thaw−pump cycles, purged with N_2, and heated at 120 °C under N_2 for 24 h. Excess *c*-octane was removed by vacuum distillation. The colorless organic distillate was added with benzene-d_6 for ^{1}H NMR spectroscopy, and *c*-octene was not observed. Degassed benzene-d_6 was added to N_2 for ^{1}H NMR spectroscopy. A red solution of Rh(tmp)H (90% yield, estimated by ^{1}H NMR spectroscopy) was obtained.

Reaction of *c*-octane with Rh^{II}(tmp) 12. Rh^{II}(tmp) (10.6 mg, 0.0012 mmol) was added to *c*-octane (1.5 mL). The red reaction mixture was degassed for three freeze−thaw−pump cycles, purged with N_2, and heated at 120 °C under N_2 for 24 h. Excess *c*-octane was removed by vacuum distillation. The colorless organic distillate was added with benzene-d_6 for ^{1}H NMR spectroscopy, and *c*-octene (40% yield, estimated by ^{1}H NMR) was observed. Degassed benzene-d_6 was added to N_2 for ^{1}H NMR spectroscopy. A red solution of Rh(tmp)H (86% yield, estimated by ^{1}H NMR spectroscopy) was obtained.

Attempted Synthesis of Rh(tmp)(*c*-octyl) 13. A suspension of Rh(tmp)Cl (20.0 mg, 0.022 mmol) in EtOH (5 mL) and a solution of $NaBH_4$ (3 mg, 0.087 mmol) in aq. NaOH (0.1 M, 0.4 mL) were purged with N_2 for 15 min separately. The solution of $NaBH_4$ was added slowly to the suspension of Rh(tmp)Cl via a cannula. The mixture was heated at 50 °C under N_2 for 1 h. The solution was then cooled to 30 °C under N_2, and *c*-octyl bromide was added. A reddish orange suspension was formed. After stirring at room temperature for another 15 min under N_2, the reaction mixture was vacuum-distilled, and the distillate went through ^{1}H NMR spectroscopy after extraction with C_6D_6/H_2O. *c*-Octene (77% yield, estimated by ^{1}H NMR) was observed. The reddish orange residue was washed with degassed H_2O (2 × 10 mL). The residue was dried by vacuum in the reaction tube, which was then protected with N_2 and brought to analytical balance. Rh(tmp)H was obtained (17.1 mg, 0.19 mmol, 89%). Degassed benzene-d_6 was added to the reddish orange residue for ^{1}H NMR spectroscopy in a sealed NMR tube.

Computational Details. Geometry optimizations were carried out with the Turbomole program package[25] coupled to the PQS Baker optimizer[26] via the BOpt package,[27] at the DFT/b3-lyp[28a−d] level (the reactions described in Scheme 6 and Table 6, using the full atom TPP models, were also evaluated at the BP86 level[28e,f]). We used the def2-TZVP basis set[29] (small-core pseudopotentials on Rh[30]) and Grimme's D3 version dispersion corrections (disp3)[31] for the geometry optimizations in all cases. All minima (no imaginary frequencies) and the transition state (one imaginary frequency) were characterized by calculating the Hessian matrix. ZPE and gas-phase thermal corrections (entropy and enthalpy, 298 K, 1 bar) from these analyses were calculated. The nature of the transition state was confirmed by IRC calculations. By calculation of the partition function of the molecules in the gas phase, the entropy of dissociation or coordination for reactions in solution is overestimated (overestimated translational entropy terms in the gas phase compared to solutions). For reactions in "solution," we therefore corrected the Gibbs free energies for all steps involving a change in the number of species. Several methods have been proposed for corrections of gas phase to solution phase data. The minimal correction term is a correction for the condensed phase (CP) reference volume (1 L mol^{-1}) compared to the gas phase (GP) reference volume (24.5 L mol^{-1}). This leads to an entropy correction term (SCP = SGP + Rln{1/24.5}) for all species, affecting relative free energies (298 K) of all associative steps of −2.5 kcal mol^{-1}.[32] Larger correction terms of −6.0 kcal mol^{-1} have been suggested based on solid arguments.[33,34] While it remains a bit debatable as to which entropy correction term is best to translate gas phase DFT data into free energies relevant for reactions in solution, in this article we adapted the suggested correction term of −6.0 kcal mol^{-1}.[33,34] For the reactions described in Scheme 6 and Table 6, using the full atom TPP models optimized at the b3-lyp level, additional dielectric constant corrections (cosmo[35]) were taken into account based on single point calculations, using the dielectric constant of benzene (ε = 2.27).

■ ASSOCIATED CONTENT

Supporting Information

Reaction progress and computational data. The Supporting Information is available free of charge on the ACS Publications website at DOI: 10.1021/acs.organomet.5b00183.

■ AUTHOR INFORMATION

Corresponding Authors

*(B.D.B.) E-mail: bdebruin@science.uva.nl.

*(K.S.C.) E-mail: ksc@cuhk.edu.hk.

Notes

The authors declare no competing financial interest.

■ ACKNOWLEDGMENTS

We thank the General Research Fund of the Research Grants Council of Hong Kong (No: 400212), The Netherlands Organization for Scientific Research, Chemical Sciences (NWO-CW VICI project 016.122.613), and the NWO/RGC Joint Research Scheme sponsored by the Research Grants Council of Hong Kong and The Netherlands Organization for Scientific Research (D-HK002/11T) for financial support.

■ REFERENCES

(1) (a) Shilov, A. E.; Shul'pin, G. B. *Chem. Rev.* **1997**, *97*, 2879−2932. (b) Crabtree, R. H. *Chem. Rev.* **1985**, *85*, 245−269.

(2) (a) Goldman, A. S. *Nature* **2010**, *463*, 435−436. (b) Park, Y. J.; Park, J.-W.; Jun, C.-H. *Acc. Chem. Res.* **2008**, *41*, 222−234. (c) Murakami, M.; Makino, M.; Ashida, S.; Matsuda, T. *Bull. Chem. Soc. Jpn.* **2006**, *79*, 1315−1321. (d) Rybtchinski, B.; Milstein, D. *Angew. Chem., Int. Ed.* **1999**, *38*, 870−883. (e) Grochowski, M. R.; Brennessel, W. W.; Jones, W. D. *Organometallics* **2011**, *30*, 5604−5610. (f) Chaplin, A. B.; Green, J. C.; Weller, A. S. *J. Am. Chem. Soc.* **2011**, *133*, 13162−13168.

(3) (a) For a heterogeneous medium, see Hagedom, C. J.; Weiss, M. J.; Kim, T. W.; Weinberg, W. H. *J. Am. Chem. Soc.* **2001**, *123*, 929−940. (b) Sawatari, N.; Yokota, T.; Sakaguchi, S.; Ishii, Y. *J. Org. Chem.* **2001**, *66*, 7889−7891.

(4) Isaacs, N. S. *Physical Organic Chemistry*; Longman: Essex, U.K., 1987.

(5) (a) For a leading reference, see Renkema, K. B.; Kissin, Y. V.; Goldman, A. S. *J. Am. Chem. Soc.* **2003**, *125*, 7770−7771. (b) Yiu, S. M.; Wu, Z. B.; Lau, T. C. *J. Am. Chem. Soc.* **2004**, *126*, 14921−14929. (c) Jiang, X. F.; Shen, M. H.; Tang, Y.; Li, C. Z. *Tetrahedron Lett.* **2005**, *46*, 487−489.

(6) Chan, Y. W.; Chan, K. S. *Organometallics* **2008**, *27*, 4625−4635.

(7) (a) Chan, Y. W.; Chan, K. S. *Chem. Commun.* **2011**, *47*, 4802−4804. (b) Chan, K. S.; Chan, Y. W. *Organometallics* **2014**, *33*, 3702−3708.

(8) (a) Wayland, B. B.; Ba, J.; Sherry, A. E. *J. Am. Chem. Soc.* **1991**, *113*, 5305−5311. (b) Zhang, X.-X.; Wayland, B. B. *J. Am. Chem. Soc.* **1994**, *116*, 7897. (c) Cui, W.; Zhang, X. P.; Wayland, B. B. *J. Am. Chem. Soc.* **2003**, *125*, 4994−4995.

(9) (a) Chan, K. S.; Chiu, P. F.; Choi, K. S. *Organometallics* **2007**, *26*, 1117−1119. (b) Choi, K. S.; Chiu, P. F.; Chan, C. S.; Chan, K. S. *J. Chin. Chem. Soc.* **2013**, *60*, 779−793.

(10) (a) Chan, K. S.; Li, X. Z.; Dzik, W. I.; De Bruin, B. *J. Am. Chem. Soc.* **2008**, *130*, 2051−2061. (b) Chan, K. S.; Chan, K. S.; Li, X. Z.; Lee, S. Y. *Organometallics* **2010**, *29*, 2850−2856.

(11) Chan, K. S.; Li, X. Z.; Fung, C. W.; Zhang, L. *Organometallics* **2007**, *26*, 2679−2687.

DOI: 10.1021/acs.organomet.5b00183
Organometallics XXXX, XXX, XXX−XXX

(12) To, C. T.; Chan, K. S. *J. Am. Chem. Soc.* **2012**, *134*, 11388−11391.
(13) Chan, Y. W.; Chan, K. S. *J. Am. Chem. Soc.* **2010**, *132*, 6920−6922.
(14) (a) Rybtchinski, B.; Vigalok, A.; Ben-David, Y.; Milstein, D. *J. Am. Chem. Soc.* **1996**, *118*, 12406−12415. (b) Perthuisot, C.; Jones, W. D. *J. Am. Chem. Soc.* **1994**, *116*, 3647−3648.
(15) Choi, K. S.; Lai, T. H.; Lee, S. Y.; Chan, K. S. *Organometallics* **2011**, *30*, 2633−2635.
(16) Dragutan, V.; Streck, R. *Catalytic Polymerization of Cycloolefins: Ionic, Ziegler-Natta and Ring-Opening Metathesis Polymerization*, 1st ed.; Elsevier: Amsterdam, The Netherlands, 2000.
(17) Wayland, B. B.; Posamik, G.; Fryd, M. *Organometallics* **1992**, *11*, 3534−3542.
(18) Wayland, B. B.; van Voorhees, S. L.; Wilker, C. *Inorg. Chem.* **1986**, *25*, 4039−4042.
(19) For the 4 centered transition state, see (a) Mak, K. W.; Chan, K. S. *J. Am. Chem. Soc.* **1998**, *120*, 9686−9687. (b) Mak, K. W.; Xue, F.; Mak, T. C. W.; Chan, K. S. *J. Chem. Soc., Dalton Trans.* **1999**, *19*, 3333−3334.
(20) Paonessa, R. S.; Thomas, N. C.; Halpern, J. *J. Am. Chem. Soc.* **1985**, *107*, 4333−4335.
(21) (a) The estimated bond dissociation energy (BDE) of (ttp)Rh-H is ∼60 kcal mol^{-1}. See ref 19. (b) The BDE of *n*-octyl-H is ∼100 kcal mol^{-1}; see Luo, Y. R. *Handbook of Bond Dissociation Energies in Organic Compounds*; CRC Press: Boca Raton, FL, 2003.
(22) (a) Davies, A. G.; Roberts, B. P. *Acc. Chem. Res.* **1972**, *5*, 387−392. (b) Johnson, M. D. *Acc. Chem. Res.* **1983**, *16*, 343−349. (c) Incremona, J. H.; Upton, C. J. *J. Am. Chem. Soc.* **1972**, *94*, 301−303. (c) Pakes, P. W.; Rounds, T. C.; Strauss, H. L. *J. Phys. Chem.* **1981**, *85*, 2469−2475. (d) Wiberg, K. B.; Waddel, S. T. J. *Am. Chem. Soc.* **1990**, *112*, 2194−2216.
(23) Haplern, J. *Acc. Chem. Res.* **1982**, *15*, 238−244.
(24) Gellrich, U.; Himmel, D.; Meuwly, M.; Breit, B. *Chem.—Eur. J.* **2013**, *19*, 16272−16281.
(25) Ahlrichs, R. *Turbomole*, version 6.5; Theoretical Chemistry Group, University of Karlsruhe: Stuttgart, Germany.
(26) PQS version 2.4, 2001, Parallel Quantum Solutions, Fayettevile, Arkansas (USA); the Baker optimizer is available separately from PQS upon request: Baker, I. *J. Comput. Chem.* **1986**, *7*, 385−395.
(27) Budzelaar, P. H. M. *J. Comput. Chem.* **2007**, *28*, 2226−2236.
(28) (a) Lee, C.; Yang, W.; Parr, R. G. *Phys. Rev. B* **1988**, *37*, 785−789. (b) Becke, A. D. *J. Chem. Phys.* **1993**, *98*, 1372−1377. (c) Becke, A. D. *J. Chem. Phys.* **1993**, *98*, 5648−5652. (d) Calculations were performed using the Turbomole functional "b3-lyp", which is not completely identical to the Gaussian "B3LYP" functional.. (e) Becke, A. D. *Phys. Rev. A* **1988**, *38*, 3098. (f) Perdew, J. P. *Phys. Rev. B* **1986**, *33*, 8822.
(29) (a) Weigend, F.; Ahlrichs, R. *Phys. Chem. Chem. Phys.* **2005**, *7*, 3297−3305. (b) Weigend, F.; Häser, M.; Patzelt, H.; Ahlrichs, R. *Chem. Phys. Lett.* **1998**, *294*, 143−152.
(30) (a) Turbomole basisset library, Turbomole version 6.5;. (b) Andrae, D.; Haeussermann, U.; Dolg, M.; Stoll, H.; Preuss, H. *Theor. Chim. Acta* **1990**, *77*, 123−141.
(31) Grimme, S.; Antony, J.; Ehrlich, S.; Krieg, H. *J. Chem. Phys.* **2010**, *132*, 154104−154119.
(32) Dzik, W. I.; Xu, X.; Zhang, P.; Reek, J. N. H.; de Bruin, B. *J. Am. Chem. Soc.* **2010**, *132*, 10891−10902.
(33) Wertz, D. H. *J. Am. Chem. Soc.* **1980**, *102*, 5316−5322.
(34) Schneider, N.; Finger, M.; Haferkemper, C.; Bellemin-Laponnaz, S.; Hofmann, P.; Gade, L. *Angew. Chem., Int. Ed.* **2009**, *48*, 1609−1613.
(35) Klamt, A.; Schüürmann, G. *J. Chem. Soc., Perkin Trans.* **1993**, *2*, 799−805.

DOI: 10.1021/acs.organomet.5b00183
Organometallics XXXX, XXX, XXX−XXX